



## Splitting of an edge dislocation by an optical vortex

D. V. PETROV

*Departamento de Química Fundamental, Universidade Federal de Pernambuco, 50670-901 Recife, PE, Brazil  
(E-mails: dvp@npd.ufpe.br, dvp@dqfex.ufpe.br)*

Received 18 December 2000; accepted 15 June 2001

**Abstract.** In a linear medium an optical vortex induces the splitting of an edge dislocation into vortices of both topological charges. Their positions and number depend on which of the phase dislocations is shifted from the center of the host beam. Violations of the charge conservation law are discussed.

**Key words:** edge phase dislocation, Gaussian beam, optical vortex, orbital angular momentum of light, phase dislocation

### 1. Introduction

Optical fields may contain topological defects of phase or phase dislocations, that is, points or lines on the wavefront surface where both the real part and imaginary part of the field vanish (Nye and Berry 1974). There are two types of phase dislocations. A screw dislocation or vortex is a spiral phase ramp around the point of phase singularity where the phase of the wave is undefined thus its amplitude must vanish. The order of the singularity multiplied by its sign is referred to as the topological charge of vortex. The doughnut mode of a laser cavity is an example of an optical vortex. An edge dislocation is the  $\pi$ -shift in the wave phase located along a line in the transverse plane. The Gauss–Hermite mode  $H_{1,0}$  is the simplest example of a field with edge dislocation.

The propagation dynamics of a vortex in both linear and nonlinear media are affected by any source of phase gradient and (or) intensity gradient, and have been the subject of numerous publications (see, for example, Basistiy *et al.* 1993, 1995; Indebetow 1993; Freund and Shvartsman 1994; Freund 1999a; Tikhonenko *et al.* 1995; Dholakia *et al.* 1996; Berzanskis *et al.* 1997; Luther-Davies *et al.* 1997; Petrov and Torner 1997, 1998; Rozas *et al.* 1997a,b; Soskin *et al.* 1997; Torner and Petrov 1997a, b; Petrov *et al.* 1998; Torner *et al.* 1998; Rozas and Swartzlander 2000). In particular, in linear media a vortex moves perpendicular to the background intensity gradient and along the background phase gradient.

Publications on the propagation dynamics of edge dislocations are few. (Basistiy *et al.* 1993, 1995; Mamaev *et al.* 1996; Tikhonenko *et al.* 1996; Ilyenkov *et al.* 1997; Kreminskaya *et al.* 1998; Vasnetsov *et al.* 1998). In particular, the nonlinear evolution of a dark stripe soliton (containing an edge phase dislocation) was studied in an anisotropic photorefractive material (Mamaev *et al.* 1996), and in a defocusing Kerr medium (Tikhonenko *et al.* 1996): at high intensities this dislocation is unstable and breaks up into pairs of vortices. Recently, Kivshar *et al.* (2000) demonstrated the vortex–dark stripe soliton interaction in a nonlinear defocusing medium. Both dislocations were created in the input beam and the beam intensity was high enough in order to achieve a soliton-type propagation of the vortex soliton and dark stripe soliton. At the output beam the soliton stripe bends and the vortex soliton itself shifts slightly. The initial distance between solitons was larger than the soliton size, therefore the long-scale interaction observed was explained by the presence of a vortex-induced phase difference. By increasing the medium nonlinearity the stripe soliton breaks up into vortices.

In a linear medium the interaction should also be observed because the amplitude- and phase-driven mechanisms of interaction between dislocations are present in this case too. The aim of this paper is to study experimentally and theoretically the interaction between two phase dislocations of different dimensionality – a vortex (2D object) and an edge dislocation (1D object) – nested in a smooth Gaussian beam by its propagation in a linear medium.

## 2. Theory

As mentioned above there are two types of wavefront dislocations. Let first review how these dislocations move when nested in a host beam. In the initial plane  $z = 0$  a field containing a single vortex embedded in a Gaussian beam of waist  $w_0$  and in general case located off of the beam maximum, can be described by an expression of the form

$$E_v(x, y, z = 0) = E_0 \left( \frac{x - x_{0v} + iy}{w_0} \right) \exp \left( - \frac{x^2 + y^2}{w_0^2} \right), \quad (1)$$

where  $E_0$  is the amplitude,  $x_{0v}$  is the shift of the vortex from the beam center. The field after propagation of a distance  $z$  is given by the Fresnel diffraction integral (Haus 1984):

$$E_v(x, y, z) = \frac{ik}{2\pi z} \iint dx' dy' E_v(x', y', z = 0) e^{i\frac{k}{2z}[(x-x')^2 + (y-y')^2]}, \quad (2)$$

where  $k$  is the wave number. Direct calculations give

$$E_v(x, y, z) = E_0 \left[ \frac{x + iy}{w_0(1 + i\xi)^2} - \frac{x_{0v}}{w_0} \frac{1}{(1 + i\xi)} \right] \exp \left[ -\frac{r^2}{w_0^2(1 + i\xi)} \right], \quad (3)$$

where  $\xi = z/(kw_0^2/2)$ . This field may contain several phase defects. Their positions can be found by equating the real and imaginary parts of the field to zero. It is well known (Rozas *et al.* 1997a; Rozas and Swartzlander 2000) that the on-axis vortex ( $x_{0v} = 0$ ) remains by propagation at the center of the host beam, however the off-axis vortex moves in a straight line, with the angular position moving clockwise (or counterclockwise) with respect to the center of the host beam.

There are different ways to represent the field of an edge dislocation nested in a Gaussian beam of waist  $w_0$ : as the Gauss–Hermite mode  $H_{1,0}$ , as a  $\tanh(x - x_{0e})$  function, or as a step function giving a  $\pi$ -shift in the wavefront at  $x = x_{0e}$ . The last two functions are best fitted to our experimental conditions (see below), however they do not allow analytical analysis of the free space propagation of the field. For this reason I chose the function

$$E_e(x, y, z = 0) = E_0 \left( \frac{x - x_{0e}}{w_0} \right) \exp \left( -\frac{x^2 + y^2}{w_0^2} \right), \quad (4)$$

to model the edge dislocation. Again using the diffraction integral (2) the field of the edge dislocation after propagation of a distance  $z$  takes the form,

$$E_e(x, y, z) = E_0 \left[ \frac{x}{w_0(1 + i\xi)^2} - \frac{x_{0e}}{w_0} \frac{1}{(1 + i\xi)} \right] \exp \left[ -\frac{r^2}{w_0^2(1 + i\xi)} \right]. \quad (5)$$

Now if the edge dislocation at  $z = 0$  is shifted from the host beam center, the field at arbitrary distance  $z$  does not contain any phase dislocation, i.e. there are no lines or points where both the real and the imaginary part of the field vanish. Hence, an edge phase dislocation is stable only if it is embedded in the center of the host beam ( $x_{0e} = 0$ ).

Having these examples of amplitude- and phase-driven vortex and edge dislocation motion as basic ideas let consider the case when at  $z = 0$  both dislocations are nested at the same Gaussian beam:

$$E(x, y, z = 0) = E_0 \frac{(x - x_{0v} + iy)(x - x_{0e})}{w_0} \exp \left( -\frac{x^2 + y^2}{w_0^2} \right). \quad (6)$$

During propagation both dislocations interact due to the mechanisms mentioned in the introduction. Obviously, the results of this interaction depend on which of the two dislocations is shifted from the host beam center because the behavior of each off-axis dislocation is different as it propagates.

### 2.1. AN ON-AXIS VORTEX, AN OFF-AXIS EDGE DISLOCATION

Let us consider an input field that consists of a single positive charge vortex, located at  $x = 0$  and  $y = 0$  ( $x_{0v} = 0$ ), and an edge dislocation located at  $x = x_{0e} = x_0$ . Calculating the diffraction integral (2) using the field given by Equation (6) one has the field  $E(x, y, z)$  after propagation of a distance  $z$ :

$$E(x, y, z) = E_0 \left[ \frac{1}{2} \frac{i\xi}{(1+i\xi)^2} + \frac{x(x+iy)}{w_0^2(1+i\xi)^3} - \frac{x_0(x+iy)}{w_0^2(1+i\xi)^2} \right] \exp \left[ -\frac{x^2+y^2}{w_0^2(1+i\xi)} \right]. \quad (7)$$

The same result was obtained using the substitution method proposed by Freund (1999b).

This field may contain several phase defects. Their positions can be found by equating the real and the imaginary parts of the field (Equation (7)) to zero. We find these to be given by

$$\begin{aligned} x_1 &= x_0 - \xi\Delta, & y_1 &= x_0\xi + \Delta; \\ x_2 &= x_0 + \xi\Delta, & y_2 &= x_0\xi - \Delta; \\ x_3 &= 0, & y_3 &= \frac{w_0^2}{2x_0}\xi; \end{aligned} \quad (8)$$

with  $\Delta = \sqrt{w_0^2/2 - x_0^2}$ .

Below I analyze positions of these vortices by changing  $x_0$  assuming that the propagation distance is constant. If  $x_0 = 0$  the output field contains two vortices  $(x_1, y_1)$  and  $(x_2, y_2)$ . The third vortex  $(x_3, y_3)$  is at infinity ( $y_3 \rightarrow \infty$ ). If  $x_0 < w_0/\sqrt{2} = x_0^*$ , the output field contains three vortices. Using the definition of vortex topological sign introduced by Freund and Shvartsman (1994) and Freund (1999a), two vortices  $(x_1, y_1)$  and  $(x_2, y_2)$  are positive (i.e. they have the same sign as the input vortex), and the sign of the third vortex  $(x_3, y_3)$  is negative. At  $x_0 = x_0^{**} = w_0\xi/\sqrt{2(1+\xi^2)}$  the vortex  $(x_1, y_1)$  collides with the vortex  $(x_3, y_3)$ , however by further increase of  $x_0$  the field con-

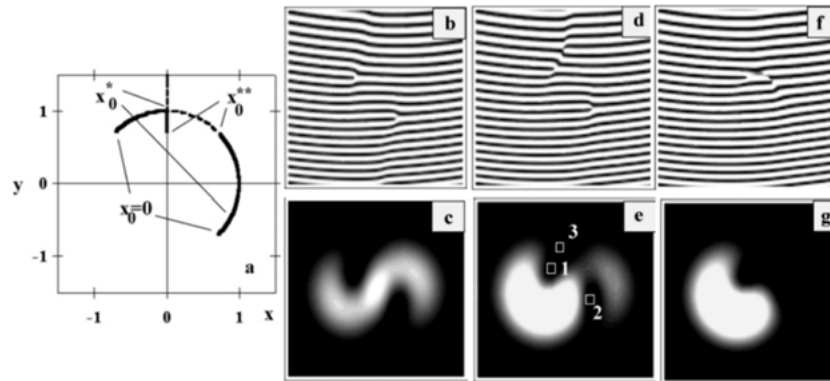


Fig. 1. Calculated trajectories of the vortices with positive (—) and negative sign (---) (a) Intensity and interferogram for different shifts of the edge dislocation  $x_0$  (b and c)  $x_0 = 0$ ,  $x_0 = 0.3$ , (f and g)  $x_0 = 0.7$ . Conditions:  $\zeta = 1$ ,  $w_0 = 1$ .

tains again three vortices. Two of them are positive and the third is negative. At  $x_0 = x_0^*$  the vortex  $(x_3, y_3)$  annihilates with the vortex  $(x_2, y_2)$ , and only one positive vortex  $(x_1, y_1)$  survives.

Fig. 1(a) shows the positions of the three vortices calculated by  $w_0 = 1$  and at  $\zeta = 1$  at different positions of the edge dislocation  $x_0$ , and Fig. 1(b–g) illustrate the intensity distributions and interference patterns, calculated from Equation (8).

At a given shift  $x_0$  the initially straight edge dislocation bends as the propagation distance increases. In the two nulls located at the bending curve a pair of screw dislocations of opposite signs appears (Fig. 2). Comparing with the nonlinear case (Kivshar *et al.* 2000), in the linear case both the amplitude gradient and the phase gradient contribute into the interaction. However the final results (the edge dislocation bending and the break up into vortices) are the same.

Fig. 3 shows the trajectories of the vortices during their propagation at a given  $x_0$ . As seen two vortices of opposite sign appear at the edge dislocation and then move along straight lines. At  $\zeta = x_0 / \sqrt{w_0^2/2 - x_0^2} = 1$  the two

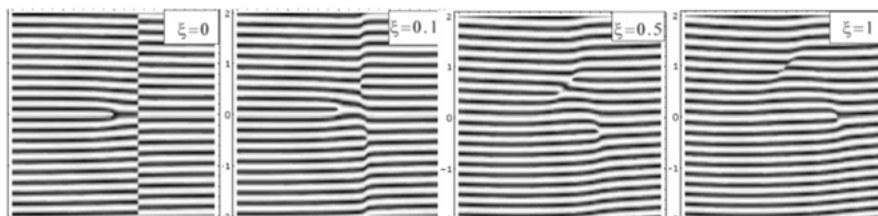


Fig. 2. Interferograms obtained at different propagation distances  $\zeta$  showing bending of the edge dislocation.  $x_0 = 0.5$ .

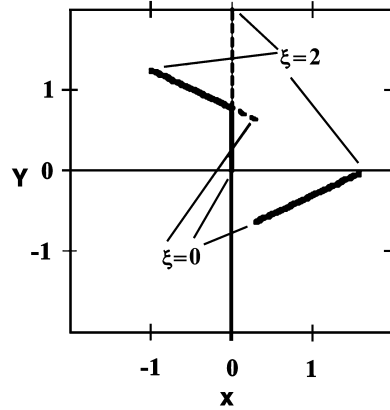


Fig. 3. Trajectories of positive (—) and negative (- - -) vortices calculated at an initial shift  $x_0 = 0.5$ .

vortices collide creating a limited edge dislocation, and by further propagation again three vortices can be observed.

Numerical simulations of the full governing equation describing the beam propagation in a linear medium in the paraxial approximation were performed with a split-Fourier algorithm (Torner and Wright 1996). I used three functions to model the edge dislocation: the Gauss-Hermite  $H_{1,0}$  function  $(x - x_0)/w_0$  as in Equation (1), the tanh-like beam  $\tanh[(x - x_0)/b]$ , where  $b$  describes the amplitude profile near  $x = x_0$ , and the step function  $\Pi(x - x_0)$ , where  $\Pi(x - x_0) = 1$  if  $x > x_0$  and  $\Pi(x - x_0) = -1$  if  $x < x_0$ , that gives a  $\pi$ -phase shift of the field at  $x = x_0$ .

The examples of numerical simulations (Fig. 4) show very good agreement with the predictions of Equation (7) within the resolution that was achievable with split-step meshes. The number of vortices and their positions are almost independent of the type of functions used to describe the edge dislocation. Hence the intensity gradient (which is different in both cases) does not contribute considerably to the interaction between the dislocations, and the phase difference generated at the edge dislocation by the vortex produces the main effect in the interaction.

One can explain the break-up of the edge dislocation and the generation of additional screw dislocations in the following simple way. The expression (6) can also be written as:

$$E(x, y, z = 0) = E_0(x^2 + ixy - xx_0 - iyx_0) \exp\left[-\frac{x^2 + y^2}{w_0^2}\right], \quad (9)$$

i.e. as a superposition of Gauss-Hermite modes  $H_{mn}(x, y)$ :  $E(x, y, z = 0) = H_{20} + iH_{11} - H_{10} - iH_{01} + H_{00}$ . As is well known the amplitude distribution of these modes has numerous intersections with zero. Therefore the condition

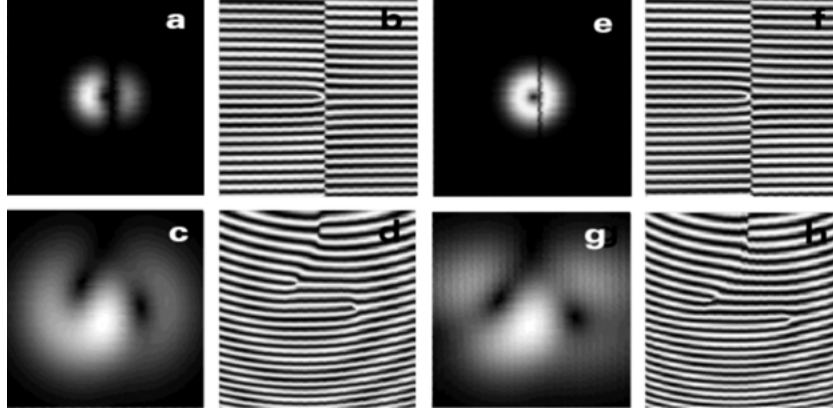


Fig. 4. Numerically obtained beam intensity distributions (a, c, e, f) and corresponding interferograms (b, d, f, h) at a fixed propagation distance  $\xi = 0$  (a, b, e, f) and  $\xi = 1$  (c, d, g, h). Plots were calculated with the edge dislocation modeled as  $(x - x_0)/w_0$  (a-d) or  $\tanh[(x - x_0)/b]$  with  $b = 0.01$  (e, h). Results found with step function  $\Pi(x - x_0)$  are not shown because they are very similar to ones obtained with  $\tanh[(x - x_0)/b]$ . Parameters:  $w_0 = 1$ ,  $x_0 = 0.3$ .

of both the real and imaginary parts vanishing can be satisfied at several points. These modes will acquire different phase shifts (proportional to the indices of the modes) upon propagation. The positions of the defects are thus not expected to remain stationary.

Therefore, the calculations based on the simple model show that the total topological charge is not conserved in free-space propagation when both phase dislocations are on-axis.

## 2.2. AN OFF-AXIS VORTEX, AN ON-AXIS EDGE DISLOCATION

Now let the edge dislocation given in Equation (6) be on-axis  $x_{0e} = 0$  but the vortex is offset of the center of the Gaussian beam. The field at  $z = 0$  is given by:

$$E(x, y, z = 0) = E_0 \frac{(x + iy - x_0)}{w_0} \frac{x}{w_0} \exp\left(-\frac{x^2 + y^2}{w_0^2}\right), \quad (10)$$

and at the distance  $z$  the field  $E(x, y, z)$  is given by

$$E(x, y, z) = E_0 \left[ \frac{1}{2} \frac{i\xi}{(1 + i\xi)^2} + \frac{x(x + iy)}{w_0^2(1 + i\xi)^3} - \frac{x_0 x}{w_0^2(1 + i\xi)^2} \right] \exp\left[-\frac{x^2 + y^2}{w_0^2(1 + i\xi)}\right]. \quad (11)$$

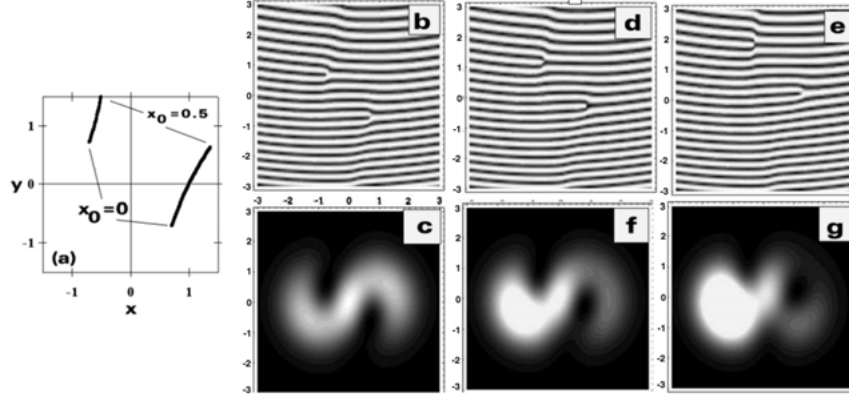


Fig. 5. Calculated positions of the vortices (a) for different initial shift  $x_0$ . Interferogram and intensity:  $x_0 = 0$  (b and c),  $x_0 = 0.3$  (d and f),  $x_0 = 0.7$  (e and g). Conditions:  $\xi = 1$ ,  $w_0 = 1$ .

This field contains two vortices at any propagation distance:

$$\begin{aligned} x_1 &= x_0/2 + \Lambda(\xi, x_0), & y_1 &= \xi \left( x_0 - \frac{w_0^2}{2x_1} \right); \\ x_2 &= x_0/2 - \Lambda(\xi, x_0), & y_2 &= \xi \left( x_0 - \frac{w_0^2}{2x_2} \right); \end{aligned} \quad (12)$$

where  $\Lambda(\xi, x_0) = \sqrt{x_0^2/4 + w_0^2 \xi^2/2}$ .

Fig. 5(a) shows the positions of the two vortices calculated by  $w_0 = 1$  and at  $\xi = 1$ , and Fig. 5(b–g) illustrates the intensity distributions and interference patterns. We see that now both vortices have the same sign as the charge of the initial vortex, hence, we again encounter a situation where the charge conservation law is violated.

Fig. 6 shows the trajectories of vortices at different  $x_0$ . At  $\xi = 0$  there is only one vortex at  $x_0$ , however by further propagation a second vortex coming from infinity moves toward the center of the host beam and then moves away. In this case the edge dislocation gives rise to just one vortex, while if the edge dislocation is initially off-axis it gives birth to two vortices with opposite charges (compare Figs. 3 and 6).

We see that the interaction between the vortex and the edge dislocation leads to different results depending on which of the two dislocations is shifted from the center of the host beam. One reason for this difference may be the following. If a Gaussian beam includes an off-axis vortex, with propagation the vortex moves along a straight line perpendicular to the intensity gradient of the host beam (Rozas *et al.* 1997a; Rozas and Swartzlander 2000). Hence, when such a vortex interacts with an edge dislocation this additional force

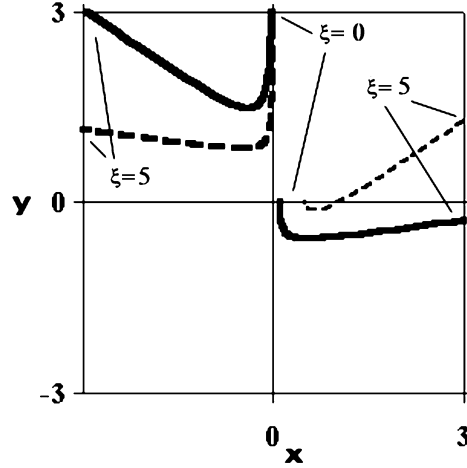


Fig. 6. Trajectories of two positive vortices calculated at two initial positions of the vortex  $x_0 = 0.1$  (—) and  $x_0 = 0.5$  (- -).

impacts the vortex's position. A on-axis vortex is always located during propagation at the center of the host beam, that is, such a vortex does not experience the effect of intensity gradient. On the other hand, if the edge dislocation alone at  $z = 0$  is shifted from the host beam center, the field at arbitrary distance  $z$  does not contain any phase dislocations. We can conclude that the edge dislocation is not stable as a phase object, and the vortex-induced perturbations of phase or (and) intensity split the edge dislocation into vortices.

Now I consider the interaction between a multiple charge vortex (in particular, with double charge) and the edge dislocation. The field at  $z = 0$  is given by:

$$E(x, y, z = 0) = E_0 \frac{(x + iy)^2 (x - x_0)}{w_0^2 w_0} \exp\left(-\frac{x^2 + y^2}{w_0^2}\right), \quad (13)$$

and after propagation of a distance  $z$  the field  $E(x, y, z)$  is:

$$E(x, y, z) = E_0 \left[ \frac{i\xi(x + iy)}{w_0(1 + i\xi)^3} + \frac{x(x + iy)^2}{w_0^3(1 + i\xi)^4} - \frac{x_0(x + iy)^2}{w_0^3(1 + i\xi)^3} \right] \exp\left[-\frac{x^2 + y^2}{w_0^2(1 + i\xi)}\right]. \quad (14)$$

This field may contain up to four vortices. Their positions are given by

$$x_1 = 0, \quad y_1 = 0;$$

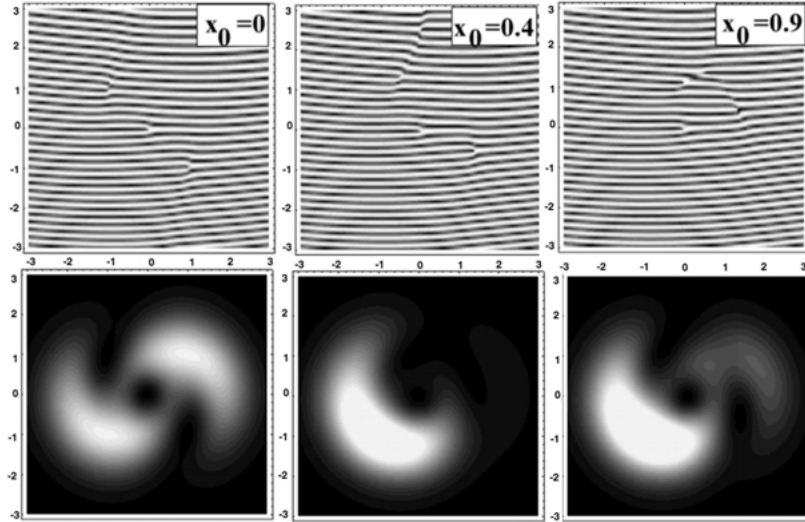


Fig. 7. Intensity and interferogram for different shift of the edge dislocation  $x_0$ . Conditions:  $\xi = 1, w_0 = 1$ , the double charge vortex.

$$x_2 = 0, \quad y_2 = \frac{w_0^2}{x_0} \xi;$$

$$x_3 = x_0 - \xi \Delta_2, \quad y_3 = x_0 \xi + \Delta_2;$$

$$x_4 = x_0 + \xi \Delta_2, \quad y_4 = x_0 \xi - \Delta_2; \quad (15)$$

with  $\Delta_2 = \sqrt{w_0^2 - x_0^2}$ . As seen, the first vortex is at the center of the host beam and its position does not change with beam propagation and does not depend on the edge dislocation position. By changing the edge dislocation shift the trajectories of the three other vortices (two of them are positive and one is negative) (Fig. 7) are very similar to those described before for the single charge vortex (Fig. 1). In this case the violation of the charge conservation law is observed if  $x_0 = 0$ .

### 3. Experiment

The experiments were designed with the following guidelines. First, only a vortex will be nested into a Gaussian beam and the phase distribution in the beam after free propagation will be monitored using an interferometric technique. Second, only an edge dislocation will be nested in the Gaussian beam and its phase structure will be also analyzed. Then, both dislocations

will be embedded in the beam and the beam's intensity and phase distributions will be studied at different initial positions of the edge dislocation relative to the vortex, which is always at the center of the Gaussian beam.

A single-charge vortex in a Gaussian beam from a He–Ne laser ( $\lambda = 0.6328 \text{ nm}$ ) was generated using an on-axis computer-generated spiral zone plate with 60 cm focal length (Heckenberg *et al.* 1992). The diameter of the mask was 0.6 cm. To separate the beam containing the vortex from the undiffracted light and high-order Fresnel images, a lens with a 10 cm focal length was placed at the fundamental focus of the zone plate. An image of the beam or an interference pattern obtained with a reference beam was observed on a screen located at about one Rayleigh length from the lens and was recorded with a charge-coupled device (CCD) camera. Fig. 8(a) and (b) shows the intensity distribution of the beam with the vortex and the corresponding interference pattern. The extra fringe generated at the phase dislocation is clearly visible.

An edge phase dislocation was created by a  $\pi$ -phase jump imposed across the beam by a thin glass plate (Mamaev *et al.* 1996; Kivshar *et al.* 2000). Interference of the reference beam with the light passing through the plate was used to adjust the tilt of the glass plate to ensure a phase shift of about  $2\pi n + \pi$  between the two halves of the beam (Fig. 8(c) and (d)). One can readily observe a one-half fringe shift of the interference fringes.

To generate both phase dislocations in the Gaussian beam the thin glass plate was introduced in the beam just before the computer-generated spiral zone plate as shown in Fig. 9. No difference in experimental results was

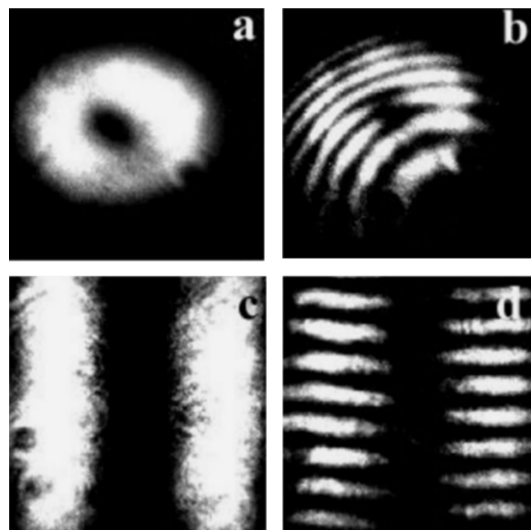


Fig. 8. Experimental images of intensity and interferogram for the output beam containing the vortex (a and b) or the edge dislocation (c and d).

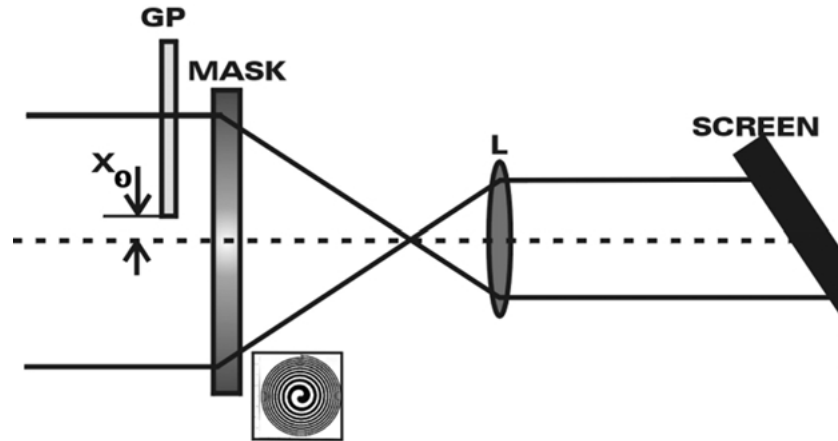


Fig. 9. Diagram of the experimental setup. *GP*, glass plate; *MASK*, computer-generated hologram; *L*, lens.

observed whether the glass plate was placed before or after the spiral zone plate. When both phase dislocations are on-axis of the host Gaussian beam ( $x_0 = 0$ ), the intensity distribution and corresponding interference pattern (Fig. 10(a) and (b)) change considerably.

Two vortices of the same topological charge (which is equal to the sign of the input vortex) appear now as a result of the interaction of the different types of phase dislocations. The edge dislocation alone is not observed. Now let the vortex be again on-axis as shown in Fig. 9, but the edge dislocation is offset to the right (the shift from the center of the vortex is about 0.1 cm). A new vortex (3) opposite in sign to other vortices (1) and (2) is observed as well

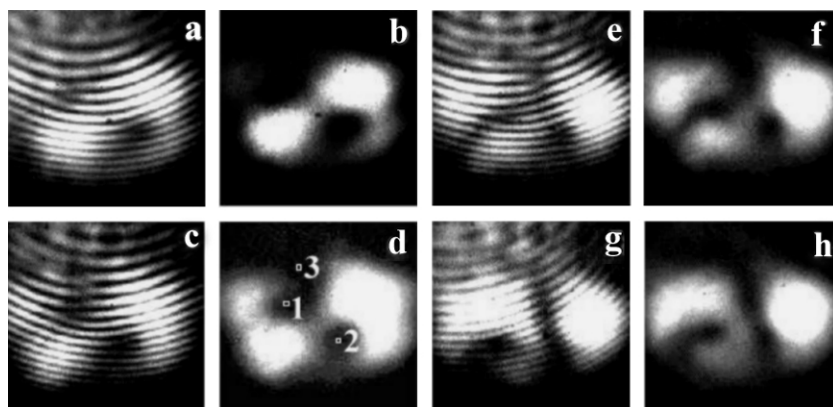


Fig. 10. Experimental images of intensity and interferogram for the output beam with the vortex and edge dislocation at different shifts of the edge dislocation  $x_0$  (a and b)  $x_0 = 0$ , (c and d)  $x_0 = 1$  mm, (e and f)  $x_0 = 2$  mm, (g and h)  $x_0 = 4$  mm.

as an asymmetry of the intensity distribution (Fig. 10(c) and (d)). By further continuous shifting of the edge dislocation the vortex (3) moves towards the vortex (1), then the vortex (3) changes its trajectory and moves towards the vortex (2) (Fig. 10(e) and (f)). At last a limited edge dislocation may be observed (Fig. 10(g) and (h)). It is notable that the vortex (1) seen in Fig. 10(c) and (d) moves downwards by the shift of the edge dislocation (compare its position in Fig. 10(g) and (h)). Comparing these plots with the numerical simulations shown on Fig. 1, the agreement between theory and experiment may give us some confidence in the model proposed.

Hence, we observed experimentally and by analytical and numerical calculations that the total topological charge is conserved (two positive vortices and one negative vortex) when the vortex is on-axis and the initial edge dislocation is off-axis. However it does not appear to be conserved when both phase dislocations are on-axis or if the edge dislocation initially is located at the beam center – two positive vortices appear in this case. The violation of topological charge conservation was mentioned for the first time by Soskin *et al.* 1997. It was shown that during free-space propagation of a light wave, which is a combination of a Gaussian beam and an optical vortex within a Gaussian envelope, additional vortices appear or annihilate. In spite of any variation in the number of vortices, the total angular momentum is constant during the propagation. Even when all vortices may be suppressed, the wavefront of the beam still has folds, but in a smooth surface without defects. These folds and not just screw phase dislocations produce components of angular momentum. Moreover, by some choices of parameters the combination of a Gaussian beam and a single charge optical vortex gives a wave with two single charge vortices of the same sign. In our case of interaction between two topological phase defects we observed a similar effect. The violation of topological charge conservation by parametric wave-mixing was observed by Petrov *et al.* 1999; Molina-Terriza *et al.* 1999.

Now let us compare these results obtained in the linear case with the nonlinear case studied by Kivshar *et al.* 2000. In the nonlinear case during propagation of each of the phase dislocations the diffraction effect is suppressed due to the nonlinear change of refractive index: they propagate as a vortex dark soliton or as a stripe dark soliton. In the linear case the diffraction is strong (compare the initial and final beam sizes in Fig. 4). Nevertheless all basic effects observed in the nonlinear case due to the interaction between the two dislocations (the stripe bending, the generation of a pair of new vortices and the shift of initial vortex) appear also in the linear case. As was mentioned in Kivshar *et al.* 2000 the main effect produced by a vortex on the dark-soliton stripe is associated with the vortex phase gradient and apparently this is correct for linear propagation also. Hence, the nonlinear objects – the vortex soliton and the dark stripe – interact in the nonlinear case in a similar manner as the vortex and the edge dislocation in a linear medium.

Probably the interaction of two phase dislocations of different dimensionality is not modified by the nonlinearities of media.

#### 4. Conclusions

The interaction of a vortex and a edge phase dislocation nested in a Gaussian beam induces nucleation of additional vortices of both topological charges. Their positions and number depend on the initial separation between these phase dislocations and on their shift from the host beam center. The total topological charge may change during beam propagation and its value may differ from the initial topological charge. The interaction between these phase dislocations may have potential practical applications such as reconfigurable beam profile modulation and multiplexing of information channels.

#### Acknowledgement

I greatly appreciate I. Freund for enlightening discussions.

#### References

- Basistiy, I.V., V.Y. Bazhenov, M.S. Soskin and M.V. Vasnetsov, *Opt. Commun.* **103** 422, 1993.  
 Basistiy, I.V., M.S. Soskin and M.V. Vasnetsov, *Opt. Commun.* **119** 604, 1995.  
 Berzanskis, A., A. Matijosius, A. Piskarskas, V. Smilgevicus and A. Stabinis. *Opt. Commun.* **140** 273, 1997.  
 Dholakia, K., N.B. Simpson, M.J. Padgett and L. Allen. *Phys. Rev. A* **54** R3742, 1996.  
 Freund, I. *Opt. Commun.* **159** 99, 1999a.  
 Freund, I. *Opt. Commun.* **163** 230, 1999b.  
 Freund, I. and N. Shvartsman. *Phys. Rev. A* **50** 5164, 1994.  
 Haus, H.A. *Waves and fields in optoelectronics*, Prentice-Hall Inc., Englewood Cliffs NJ, 1984.  
 Heckenberg, H.R., R. McDuff, C.D. Smith and A.G. White. *Opt. Lett.* **17** 221, 1992.  
 Ilyenkov, A.V., L.V. Kreminskaya, M.S. Soskin and M.V. Vasnetsov. *J. Nonlinear Opt. Phys.* **6** 169, 1997.  
 Indebetouw, G. *J. Mod. Optics* **40** 73, 1993.  
 Kivshar, Y.S., A. Nepomnyashchy, V. Tikhonenko, J. Christou and B. Luther-Davies. *Opt. Lett.* **25** 123, 2000.  
 Kreminskaya, L.V., M.S. Soskin, A.I. Khizhnyak. *Opt. Commun.* **145** 377, 1998.  
 Luther-Davies, B., J. Christou, V. Tikhonenko and Y.S. Kivshar. *J. Opt. Soc. Am. B* **14** 3045, 1997.  
 Mamaev, A.V., M. Saffman and A.A. Zazulya. *Phys. Rev. Lett.* **76** 2262, 1996.  
 Molina-Terriza, G., L. Torner and D.V. Petrov. *Opt. Lett.* **24** 899, 1999.  
 Nye, J.F. and M. Berry. *Proc. R. Soc. London A* **336** 165, 1974.  
 Petrov, D.V. and L. Torner. *Opt. Quantum Electron* **29** 1037, 1997.  
 Petrov, D.V. and L. Torner. *Phys. Rev. E* **58** 7903, 1998.  
 Petrov, D.V., G. Molina-Terriza and L. Torner. *Opt. Commun.* **162** 357, 1999.  
 Petrov, D.V., L. Torner, J. Martorell, R. Vilaseca, J.P. Torres and C. Cojocaru. *Opt. Lett.* **23** 1444, 1998.  
 Rozas, D. and G.A. Swartzlander. *Opt. Lett.* **25** 126, 2000.  
 Rozas, D., C.T. Law and G.A. Swartzlander. *J. Opt. Soc. Am. B* **14** 3054, 1997a.

- Rozas, D., Z.S. Sacks and G.A. Swartzlander. *Phys. Rev. Lett.* **79** 3399, 1997b.
- Soskin, M.S., V.N. Gorshkov, M.N. Vasnetsov, J.T. Malos and N.R. Heckenberg. *Phys. Rev. A* **56** 4064, 1997.
- Tikhonenko, V., J. Christou and B. Luther-Davies and Yu.S. Kivshar. *Opt. Lett.* **21** 1129, 1996.
- Torner, L. and D.V. Petrov. *J. Opt. Soc. Am. B* **14** 2017, 1997a.
- Torner, L. and D.V. Petrov. *Electron. Lett.* **33** 608, 1997b.
- Torner, L. and E.M. Wright. *J. Opt. Soc. Am. B* **13** 864, 1996.
- Torner, L., J.P. Torres, D.V. Petrov and J.M. Soto-Crespo. *Opt. Quantum Electron* **30** 809, 1998.
- Vasnetsov, M.V., I.V. Basistiy and M.S. Soskin. *Proc. SPIE* **3487** 29, 1998.